To appear in *Mater. Sci. Forum* (2002)

# Residual Strain Evolution during the Deformation of Single Fiber Metal Matrix Composites

Jay C. Hanan[1], Ersan Üstündag[1,*], Bjørn Clausen[1], Mahesh Sivasambu[2], Irene J. Beyerlein[2], Donald W. Brown[3], Mark A. M. Bourke[3]

[1] Department of Materials Science, M/C 138-78, California Institute of Technology Pasadena, CA 91125, USA

[2] Theoretical Division and [3] Materials Science and Technology Division, Los Alamos National Laboratory, Los Alamos, NM 87545, USA

**Keywords:** Metal matrix composites, thermal residual stress, fiber failure, $Al/Al_2O_3$ composite.

**Abstract.** Successful application of metal matrix composites often requires strength and lifetime predictions that account for the deformation of each phase. Yet, the deformation of individual phases in composites usually differs significantly from their respective monolithic behaviors. An approach is presented that quantifies the deformation parameters of each phase using neutron diffraction measurements before, during, and after failure under tensile loading in model composites consisting of a single alumina fiber embedded in an aluminum matrix. The evolution of residual strains after loading was examined including the effects of fiber failure.

## Introduction

The nucleation and interaction of fiber fractures is a primary factor in the strength and lifetime of fiber composites. These fractures unload onto neighboring fibers and matrix, generating strain concentrations that promote more fiber breaks. The magnitudes and length scales of the strain concentration fields depend on the response of the matrix and interface. Therefore, knowledge of the *in-situ* constitutive behavior of these regions is crucial for determining internal stress states [1].

Neutron diffraction is an ideal tool for the examination of bulk strains in a composite material under stress. Elastic lattice strains may be independently monitored revealing the elastic *in-situ* behavior. With the aid of micromechanical models verified by the lattice strains, the constitutive behavior may be understood.

The phase specific elastic lattice strains of a single fiber metal matrix composite were examined with reference to the residual strain in the composite. The composite was stressed to the point of fiber failure. The resulting change in residual strains was examined providing information on matrix and interface behavior.

## Experimental Procedure

The model composite comprised of a single, polycrystalline alumina fiber (4.75 mm diameter, from Coors Ceramics, Golden, CO) and an aluminum alloy, A356 (Temco (TsT) Fontana, CA), matrix prepared by casting. In order to engineer fiber fracture at the center of the gage section, a 0.4 mm notch was cut around the circumference of the fiber to a depth of 1.1 mm using a diamond saw. The composite was cast horizontally in a graphite mold. For optimum matrix properties, following room temperature aging of 16 hours, the composite was heat treated for 8 hours at 155°C. A cylindrical tensile sample was then machined from the cast form. The final dimensions of the sample gave a 30 mm long gage length with an 8.25 mm total diameter.

Mechanical loading and residual strain experiments with simultaneous neutron diffraction were performed using the Neutron Powder Diffractometer (NPD) and the Spectrometer for MAterials

* Corresponding author; electronic mail: ersan@caltech.edu.

Research at Temperature and Stress (SMARTS) [2] instruments at the Los Alamos Neutron Science Center (LANSCE). An Instron hydraulic load frame stressed the composite under load control holding for approximately 45 min. per loading step.

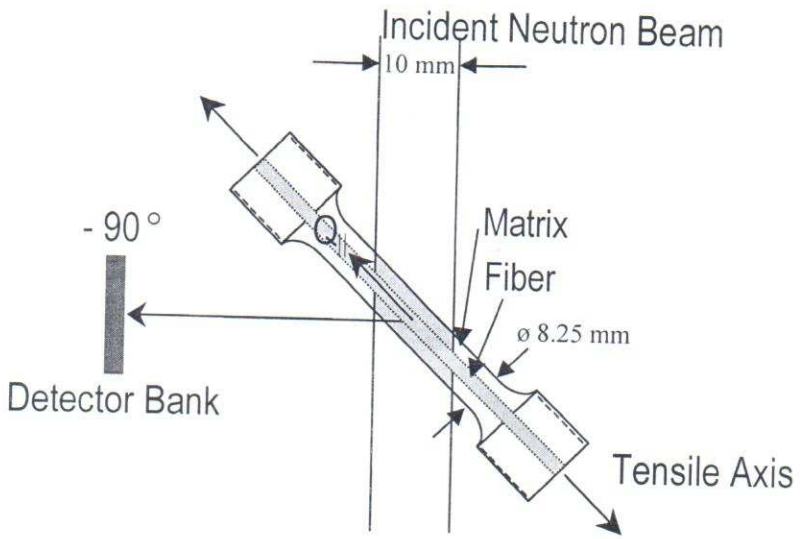


**Figure 1.** Schematic of the single fiber composite test specimen. Longitudinal strains measured in the –90° detector bank are integrated over the area irradiated by the incident neutron beam.

Using time-of-flight neutron diffraction, the bulk average elastic lattice strain is obtained in both the longitudinal and transverse directions simultaneously. A schematic revealing the $2\theta = -90°$ detector bank as it relates to the sample and beam positions is shown in Fig. 1. As shown by the Q vector, data binned from this bank provides longitudinal strain from both the fiber and the matrix. The strains are an average over the 14 mm neutron gage length created by a 10 mm wide neutron beam, which illuminates the entire width of the sample at an incident angle of 45°.

Using SMARTS, some measurements were also performed with a smaller sampling volume. The beam size was reduced to 3 mm wide by 10 mm high and radial collimators were inserted in front of the detectors. The radial collimators further limited the sampling volume to 3 mm along the beam direction. Since the sample may be translated along its axis, the smaller sampling volume adds the ability to determine variations in the strains along the fiber axis. Five neighboring positions along the fiber axis centered along the sample gage length were examined before and after loading the composite. The change in lattice parameter for these positions gives the change in residual strain along the axis of the composite.

Phase specific elastic strain was determined from the diffraction data via the Rietveld method [3]. The lattice parameter, $a$, for each phase in the gage length was determined from each constant load scan. The strain is determined directly from the change in lattice parameter of each phase at each load according to [($a$ observed)-($a$ reference)] / ($a$ reference). Along with the information from diffraction, total macroscopic strain was measured on the surface of the samples using a 25 mm gage length extensometer. When the reference lattice parameter is set to a stress free value, diffraction provides the elastic residual strain. Optionally the thermal residual strains may be subtracted from the reference lattice parameter so that the fiber and matrix strains may be compared against a common origin (as in Figs. 2 and 3).

In order to obtain the stress free lattice parameter, reference specimens were required. The stress free A356 specimens were prepared according to the same method as the composite samples except the fiber was left out of the mold. For the fiber reference, the matrix was removed from the gage section of a standard composite sample. The common processing environment ensures a common microstructure for the composite and references.

Sample displacement from the diffractometer center may be interpreted as strain [4]. To avoid this error, a sample holder was designed so that the reference specimens and the composite could be analyzed sequentially from the same position in the beam. Displacement was minimized by optically verifying the position of the sample using precision alignment telescopes associated with the SMARTS instrument. Translation to sequential samples was automated facilitating a measurement of precision. Each sample was rotated through the specimen holder three times and the statistical variation of residual strains was recorded.

**Results and Discussion**

Since the matrix's coefficient of thermal expansion (CTE) is greater than the fiber's, a residual stress state of axial compression is expected in the fiber balanced by axial tension in the matrix after processing. Averaged over 14 mm of the gage section, the axial compressive strain in the fiber was $-540 \pm 40 \times 10^{-6}$ strain and the axial tensile strain in the matrix was $+1460 \pm 30 \times 10^{-6}$ strain. Inserting these residual strains into the concentric cylinder model [5], the change in temperature required to cause the observed residual strains as well as the resulting residual stresses may be determined. This change in temperature results in a stress free temperature or "freezing temperature" for residual strains which was no greater than 150 °C, an expected result following the heat treatment. The axial stresses in the fiber and matrix predicted by the concentric cylinder model were –210 MPa and +100 MPa respectively. The monolithic aluminum reference alloy began to yield after $760 \times 10^{-6}$ strain. Assuming the monolithic constitutive behavior remained valid for the matrix, due to the CTE mismatch, plastic strain must have occurred in the matrix as the composite cooled. Therefore, with application of load further plastic yielding was expected to occur immediately in the matrix.

Also due to CTE mismatch, a residual *transverse* compressive stress exists in the fiber. However, since the entire circumference is averaged by the neutron beam, the radial and hoop strains cannot be separated analytically [6]; thus, the magnitude of compression in the radial direction is unavailable with this experimental setup. Independent of magnitude, this stress state increases the friction or clamping force on the fiber at the interface.

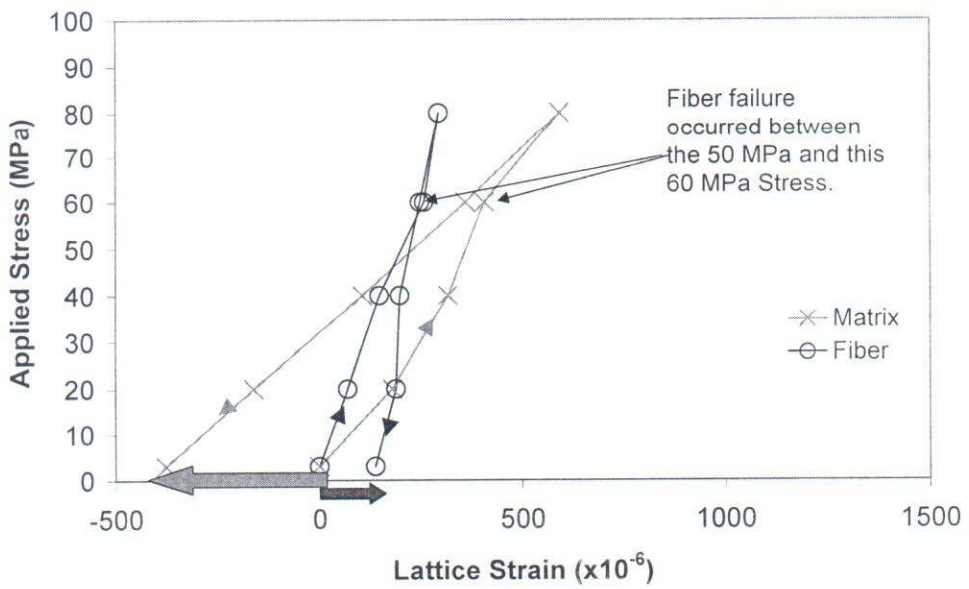


**Figure 2.** The progression of residual strains relative to the as-processed state averaged over a 14 mm length (3 fiber diameters) of the composite. The fiber broke at the notch leaving the matrix intact. The evolution of residual strain is marked by the thick arrows. Relative to the initial unloaded strain, the fiber evolved a less compressive state and the matrix a less tensile state.

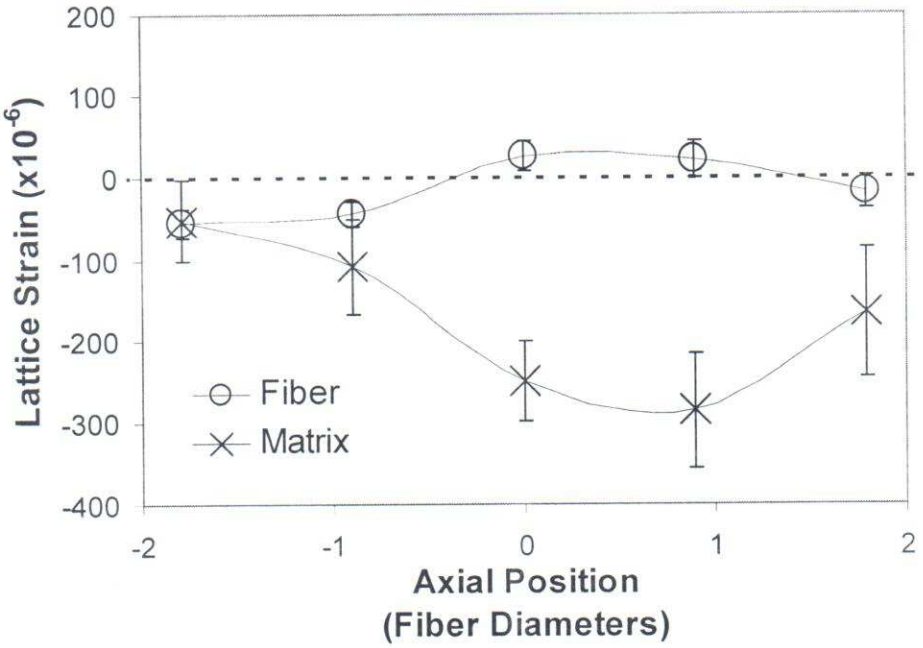


**Figure 3.** The *change* in axial elastic residual strains after one loading cycle as a function of axial position in the composite is shown (fiber diameter = 4.75 mm). The fiber failure occurred between the 0 and +1 axial position. Each position represents strains from the 3 x 10 x 3 mm neutron sampling volume referenced to the strains at each position before the loading cycle.

Since the fiber was engineered to fail before the matrix, the composite could be unloaded in the beam after fiber failure allowing the evolution of residual strains to be revealed by neutron diffraction. If the interface remains intact, then the fiber will carry most of the load. Thus, since the fiber is much stiffer than the matrix, large strains in the matrix were not expected until fiber failure. Several samples showed this behavior [7]. The observed changes in residual strains in the composite following fiber failure (see Figs. 2-3) appear to originate from plastic deformation in the matrix.

The stress/strain curves have been compared to predictions from finite element and analytical models [6]. The comparisons suggest a small zone of plastic deformation is required around the break in order to obtain the observed behavior. The plastic zone is expected to grow in the radial and axial directions away from the fiber break. However, as the radius increases, the stress decreases keeping the plastic zone to about less than 10% of the diffracting volume for applied stresses up to 100 MPa. Therefore, the measured elastic strains account for the majority of the strains present in the composite.

As the composite was loaded, the matrix locally yielded and transferred load to the fiber. Eventually, as the composite approached 60 MPa, the fiber failed. The change in slope of the fiber strains in Fig. 2 confirmed the failure. Also confirming the fiber failure was the non-linear increase in strain observed from the extensometer as the load exceeded 60 MPa. The effects of the deformation region propagate along the fiber during loading, but it was not until unloading where the evolution of residual strains made clear the magnitude of these effects. The effect of the fiber failure was observed 1.9 fiber diameters from the failure in each direction altering the elastic residual strains for 9 mm along the gage length (Fig. 3). Even without the evidence from Fig. 2, the residual strain evolution in Fig. 3 confirms the fiber failed during loading of the composite. Therefore, for this composite system, solely an analysis of the change in residual strain is sufficient to determine the presence of fiber failure.

## Conclusions

Using the phase specific elastic lattice strains given by neutron diffraction in a single fiber metal matrix composite, the residual strains were examined. The composite was stressed to the point of fiber failure. The resulting change in residual strains showed the effects of fiber failure were contained to within two fiber diameters of the failure plane.

The absolute elastic residual strains were also identified in the single fiber metal matrix composite using neutron diffraction. The matrix was shown to be in an average state of axial tension at least two times its monolithic elastic limit. The fiber was in an opposing residual compressive state, which agreed with the thermal history of the composite. For this composite, the evolution of residual strain was shown to be an effective indicator of fiber fracture and matrix plasticity.

## Acknowledgements

The aluminum was provided by Bob Frick of Temco (TsT) Fontana, CA. Important modifications of equipment and design of new tools benefited from the skills of Thomas Cisneros from the Lujan Center, LANSCE. Lujan Center is part of a national user facility supported by the Department of Energy under contract W-7405-ENG-36. Funding at Caltech was provided by the National Science Foundation (CAREER grant no. 9985264) and a Laboratory-Directed Research and Development Project (no. 2000043) at Los Alamos.

## References

[1] J. C. Hanan, I. J. Beyerlein, E. Üstündag, G. A. Swift, B. Clausen, D. W. Brown, M. A. M. Bourke, *Adv. in Fracture Research ICF* **10**, Elsevier, UK (2001).
[2] M. A. M. Bourke, E. Üstündag and D. C. Dunand, unpublished (2001).
[3] A. C. Larson, R. B. von Dreele, *GSAS-General Structure Analysis System*, LAUR 86-748, Los Alamos National Laboratory (1986).
[4] I. C. Noyan, J. B. Cohen, *Residual Stress*, Springer-Verlag New York Inc.: New York, (1987).
[5] B. Budiansky, J. W. Hutchinson and A. G. Evans, *J. Mech. Phys. Solids* **34** (1986), p. 167.
[6] J. C. Hanan, M. Sivasambu, I. J. Beyerlein, E. Üstündag, B. Clausen, D. W. Brown, M. A. M. Bourke, to be submitted to *Acta. Mater.* (2002).
[7] J. C. Hanan, E. Üstündag, I. J. Beyerlein, G. A. Swift, B. Clausen, D. W. Brown, M. A. M. Bourke, *Adv. X-Ray Anal.* **45** (2002).